Bulletin of the Seismological Society of America, Vol. 102, No. 6, pp. 2704–2713, December 2012, doi: 10.1785/0120120047

Estimation of Peak Ground Acceleration from Horizontal Rigid Body Displacement: A Case Study in Port-au-Prince, Haiti

by Susan E. Hough, Tomoyo Taniguchi, and Jean-Robert Altidor

Abstract The *M* 7.0 Haiti earthquake of 12 January 2010 caused catastrophic damage and loss of life in the capital city of Port-au-Prince. The extent of the damage was primarily due to poor construction and high population density. The earthquake was recorded by only a single seismic instrument within Haiti, an educational seismometer that was neither bolted to the ground nor able to record strong motion on scale. The severity of near-field mainshock ground motions, in Port-au-Prince and elsewhere, has thus remained unclear. We present a detailed, quantitative analysis of the marks left on a tile floor by an industrial battery rack that was displaced by the earthquake in the Canape Vert neighborhood in the southern Port-au-Prince metropolitan region. Results of this analysis, based on a recently developed formulation for predicted rigid body displacement caused by sinusoidal ground acceleration, indicate that mainshock shaking at Canape Vert was approximately 0.5*g*, corresponding to a modified Mercalli intensity of VIII. Combining this result with the weak-motion amplification factor estimated from aftershock recordings at the site as well as a general assessment of macroseismic effects, we estimate the peak acceleration to be $\approx$0.2*g* for sites in central Port-au-Prince that experienced relatively moderate damage and where estimated weak-motion site amplification is lower than that at the Canape Vert site. We also analyze a second case of documented rigid body displacement, at a location less than 2 km from the Canape Vert site, and estimate the peak acceleration to be approximately 0.4*g* at this location. Our results illustrate how observations of rigid body horizontal displacement during earthquakes can be used to estimate peak ground acceleration in the absence of instrumental data.

Introduction

The *M* 7.0 Haiti earthquake occurred at 21:53 UTC (16:53 local time) on 12 January 2010, with an epicenter near the town of Leogane, approximately 25 km west of Port-au-Prince. The epicenter is almost directly along the mapped trace of the Enriquillo Plaintain Garden fault (EPGF), the primary plate boundary fault in southern Haiti (e.g., Mann *et al.*, 1991; Calais *et al.*, 2002). Analysis of available data, including regional seismic, Global Positioning System (GPS), and Interferometric Synthetic Aperture Radar (InSAR) data, has yielded several different mainshock rupture models (Calais *et al.*, 2010; Hayes *et al.*, 2010). Although the models differ in detail, all involve moment release on a north-dipping fault adjacent to the EPGF and a predominantly unilateral rupture toward the west, although fault rupture with relatively minor moment release is inferred to have extended 5–10 km east.

The earthquake caused catastrophic damage and loss of life in Port-au-Prince. A massive building assessment program undertaken in the months following the earthquake revealed that 52% of the houses were safe for habitation, 26% could be made safe with repairs, and 21% were in need of major repair or demolition (Miyamoto *et al.*, 2011). Some parts of the city were more heavily damaged than others, but no corner of the metropolitan region escaped unscathed, with generally moderate damage throughout the mapped tan areas in Figure 1a. (The damage characterization was derived from the analysis of remote-sensing data, as described by Voigt *et al.*, 2011.) The overall scale and scope of the damage suggested severe mainshock ground motions. However, it is clear that the catastrophic extent of the damage from this earthquake was largely due to the prevalence of poor construction.

Although the 2010 earthquake was well recorded at teleseismic and regional distances, it was not recorded by any strong-motion instruments in Haiti. The severity and distribution of mainshock ground motions in the metropolitan Port-au-Prince region thus remains very poorly constrained. Faced with the near certainty of a future earthquake on the EPGF system east of the 2010 mainshock (e.g., closer to Port-au-Prince), two key questions emerge: (1) What level of

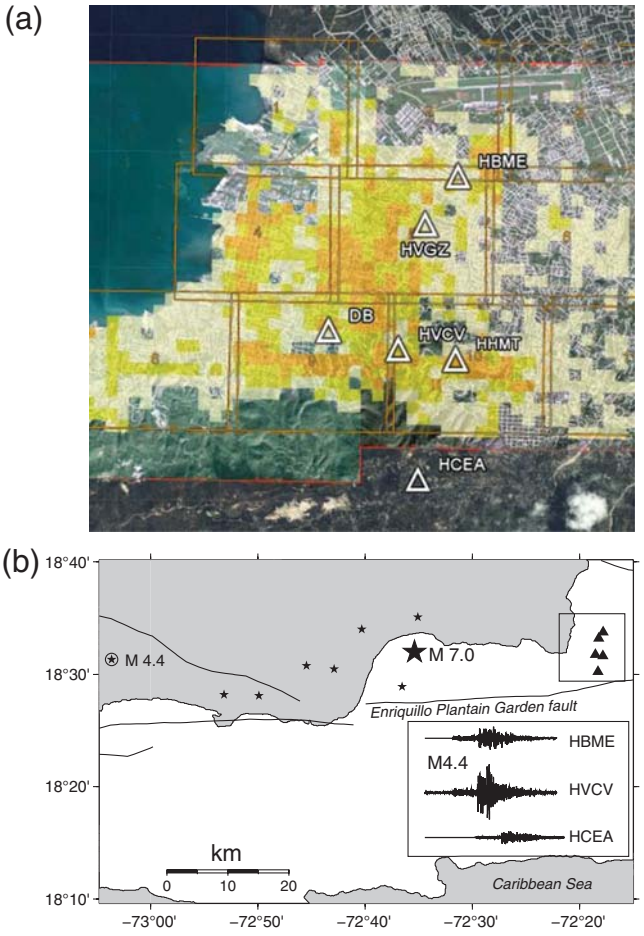

Figure 1. (a) Damage distribution for the mainshock determined from analysis of remote-sensing imagery (Voigt *et al.*, 2011). Colors indicate estimated percent building damage: 0%–10% (tan), 10%–40% (yellow), and > 40% (orange). Portable seismic stations are also shown (white triangles): foothill stations HVCV and HHMT, reference station HCEA, and valley stations HBME and HVGZ. The house shown in Figure 2b is close to the location of HVGZ. The location of the Digicel Building (DB) is also indicated by a white triangle. (b) Approximate epicenter of the 12 January 2010 earthquake is indicated by a large star; portable stations deployed to record aftershocks are shown by triangles; the inset panel shows the north–south (NS) component of motion at stations HBME, HVCV, and HCEA for the *M* 4.4 aftershock on 21 September 2010 (circled star); and the mapped trace of the EPGF is shown along with other mapped faults. The peak acceleration at HVCV is 0.08*g*. Area of damage map shown in (a) corresponds to the inset box in the upper right.

shaking could occur during a future earthquake, and how does the predicted shaking compare with that during the 2010 mainshock? (2) Does shaking severity vary significantly throughout the Port-au-Prince metropolitan area due to local geological structure?

Although no mainshock recordings are available from Port-au-Prince, weak-motion amplification factors have been determined from aftershocks recorded on eight portable digital strong-motion instruments that were deployed in March 2010 to explore the variability of ground-motions across the urban area (Fig. 1; Hough *et al.*, 2010). Two stations, HVCV and HHMT, were installed at foothill sites, where local geological conditions were expected to be intermediate between the hills to the south and the valley to the north (Fig. 1a). The instruments were installed at a cell phone facility owned by the Voila Corporation and the Hotel Montana, respectively. Analysis of the aftershocks recorded across the array revealed that inferred amplification was higher at these two stations than at adjacent stations in the valley. The results of this investigation are presented by Hough *et al.* (2011), who concluded that the amplification at HHMT and HVCV is due to topographic effects (e.g., Sanchez-Sesma, 1985), and will be used in this study to explore mainshock ground motions.

In the absence of instrumental strong-motion data, careful analysis of macroseismic effects can be useful in determining ground motion parameters including peak ground acceleration (PGA) and peak ground velocity (PGV; e.g., Atkinson and Wald, 2007). Macroseismic intensities for the Haiti earthquake were determined from a total of almost 1000 reports submitted to the Community Internet Intensity Map ("Did You Feel It?") site (Wald *et al.*, 1999). A total of 15 accounts were submitted from Port-au-Prince, from which an average numerical intensity of 7.4 was determined. It is not known where within the city the accounts were from; the overall damage distribution (Fig. 1a) suggests significant variability in the damage and shaking across the metropolitan region. Of note for this study, the northern metropolitan region, where HBME and HVGZ were located, experienced significant but less pervasively severe damage than the parts of the city to the west-southwest. In the southern metropolitan region, a band of severe damage occurred along the foothills, where HHMT and HVCV were located. The Voight *et al.* (2011) damage assessment does not extend into the residential areas to the south, including in LaBoule where HCEA was deployed. Damage in this region was generally light.

A thorough, systematic survey of seismic intensities, properly taking vulnerability into account, has not been done to date. A handful of well-documented direct eyewitness accounts suggest relatively moderate shaking severity. For example, a direct eyewitness survey revealed that, in the apparently well-built commercial structure shown in Figure 2a, shaking severity was a modified Mercalli intensity (MMI) of V: some small objects overturned, no cracks or structural damage, pictures hung on nails knocked askew but not off of the walls, etc. The buildings on both sides of this structure collapsed catastrophically. Similarly, the house shown in Figure 2b, which can reasonably be assumed to be of ordinary masonry construction and workmanship, neither reinforced nor designed to resist lateral forces, sustained only minor surficial cracks and some toppling of unsecured objects, indicating MMI VI. Many nearby structures, including a school building directly adjacent to the house, sustained catastrophic damage or collapse.

The severity of mainshock ground motions was considered by Goodno *et al.* (2011), who evaluated the performance of mechanical and electrical systems of selected critical

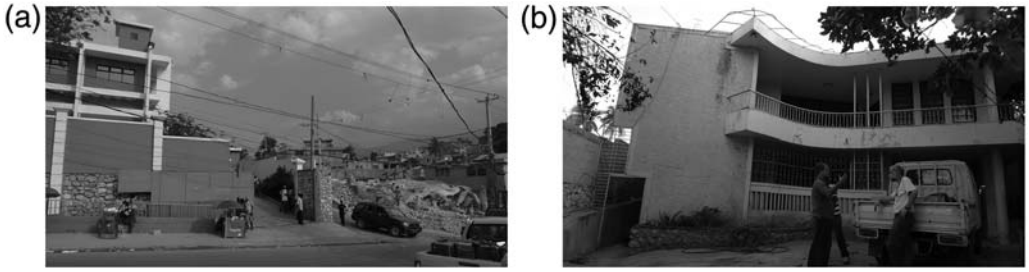

Figure 2. (a) A good-quality commercial structure in which MMI V–VI is estimated based on an eyewitness interview. (b) A private home, masonry C construction for which MMI VI is estimated. The structures on both sides of the structure shown in (a) collapsed catastrophically, as did a school building adjacent to the house shown in (b).

facilities at ten sites located between 13 and 22 km of the mainshock epicenter. Goodno *et al.* (2011) obtained rough estimates of PGA based on general correlations established from damage observations from the 1971 San Fernando, California, earthquake and from established associations between MMI and PGA. They estimated 0.13–0.2, 0.15–0.3, and 0.3–0.47*g* at sites that experienced light, moderate, and major damage, respectively.

To investigate the severity of mainshock shaking quantitatively, we use a recently developed formulation for the predicted displacement of a rigid body in response to an input sinusoidal acceleration (Taniguchi and Miwa, 2004, 2007). The displacement of a rigid body subjected to horizontal accelerations was first investigated by Newmark (1965). Choi and Tung (2001) re-derived this formula in terms of the displacement response spectrum. A small number of forensic studies, that is, analysis of observed displacement to infer PGA, have been done. For example, in a report by the Ministere de l'Ecologie, du Developpement et de l'Amenagement Durable (Ministere de l'Ecologie, du Developpement et de l'Amenagement Durable (MEDAD), 2007), Newmark's formulation is applied to estimate PGA based on observed displacement of tombstones during an M 6.8 earthquake in Japan. Related studies have focused on the estimation of PGA based on observations of toppled artifacts such as free-standing columns; these studies focus on the rocking rather than the sliding response of rigid bodies (e.g., Hinzen, 2009). To the best of our knowledge, the improved formulation of Taniguchi and Miwa (2007) has not been used previously to estimate PGA based on observed rigid body displacement. We employ the approach in this study to analyze two specific cases documented following the 2010 Haiti earthquake: HVCV and a second site located approximately 2 km west of this location, and the commercial Digicel Corporation building (Fig. 1a) investigated by Goodno *et al.* (2011). We consider the results of our quantitative analyses in light of the weak-motion amplification observed at HVCV and the generalized assessment of shaking severity by Goodno *et al.* (2011). We further consider the implications of these results for the assessment of the overall severity and distribution of shaking in the Port-au-Prince metropolitan area. We note that some studies have concluded that, as a single parameter, PGV correlates with damage better than PGA (e.g., Bommer and Alarcon, 2006). However, we focus on PGA in this study because the formulation of Taniguchi and Miwa (2007) is based on acceleration and in order to facilitate comparison with the results of other studies.

Shaking Intensity at Canape Vert (HVCV)

In this study, we focus on a unique case of documented horizontal rigid body displacement at HVCV. The apparently well-built, well-engineered two-story building at this site sustained little structural damage (Fig. 3a). On the grounds of the cell phone facility, a retaining wall and part of the parking lot collapsed (Fig. 3b), and cinderblock walls fell. Interviews with employees who were in the building at the time reveal that shaking within the building was strong enough to topple computer monitors, free-standing counters,

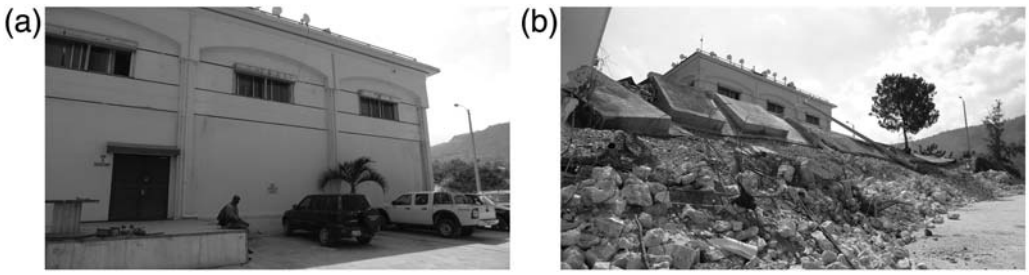

Figure 3. (a) Canape Vert Voila cell phone facility. (b) Collapse of the retaining wall in the parking lot. The face of the building seen in the photograph is aligned roughly north–south; the battery racks discussed in this study are located on the ground floor in a large room behind the doors seen in (a).

Figure 4. Damage to a recently constructed commercial building approximately 0.5 km west of HVCV. The building was later demolished.

and other furniture, and to knock people to their feet several times when they tried to run. Employees also reported that the building itself sustained light damage to the upper right corner, which is visible in Figure 3a; the extent of the damage, which had been repaired by March 2010, is not clear.

In the residential neighborhood just west of HVCV, almost all houses collapsed catastrophically. All of these structures, however, were unreinforced masonry of extremely poor construction. Within approximately 0.5 km of HVCV, a recently completed, apparently well-built commercial structure sustained substantial damage (Fig. 4). This structure was not salvageable, and by November 2010 it had been demolished.

At HVCV, shaking was strong enough to displace heavy industrial battery racks on the ground floor of the Voila building shown in Figure 3a. The battery rack shown in Figure 5 was one of several rows of similar racks in two large rooms on the ground floor of the northwest side of the building (Fig. 6). Two of the racks had been moved by the earthquake; the one shown in the foreground of Figure 5a (hereinafter called rack S) experienced the most displacement and left the most clear and accessible marks on the floor. The rack to the immediate north of rack S, hereinafter called rack N, was also displaced. Nearby apparently identical racks remained in their original positions. Each of these racks holds a total of 24 batteries: six rows of four. Each battery weighs approximately 145 kg; the weight of the batteries is thus approximately 3490 kg. The rack is 141 cm long, 172 cm tall, and 56 cm wide including the full width of the feet and approximately 40 cm without the feet. The height/width aspect ratio is thus approximately 3:1.

The close-up photograph of the floor near the rack (Fig. 5a) reveals two adjacent holes where two adjacent racks were anchored. Rack S was initially set into motion toward the south; the neighboring rack, rack N, moved toward the north. From our field observations, it appears that the bolt holding down rack N was broken, whereas the bolt holding down rack S was pulled out of the floor. Two intact bolts were found on the floor: one bent and one straight with its expansion sheathing still intact. We develop the following scenario to explain how the racks responded to the shaking: (1) two aligned bolts holding down the north side of rack S were improperly installed, perhaps due to a weak seam in the concrete beneath the tile; (2) initial strong motion produced an overturning moment that was not strong enough to break the bolts holding down other racks in the room but was strong enough to pull out the two improperly installed bolts; (3) once the bolts were pulled out, the rack experienced an especially strong rocking response; (4) as rack S rocked back to the north, it collided with rack N, which had experienced a less severe rocking response; (5) the force of the collision broke the bolts holding down rack N, allowing it to move to the north; and (6) as a result of the collision, rack S moved initially to the south.

It is possible to calculate the acceleration that would have been required to break the bolts. From our inferred scenario, including the observation that similar racks in the room were not displaced, this calculation can only provide an upper bound on ground-motion severity. We return to this calculation later. First, we focus on an interpretation of the documented displacement of rack S.

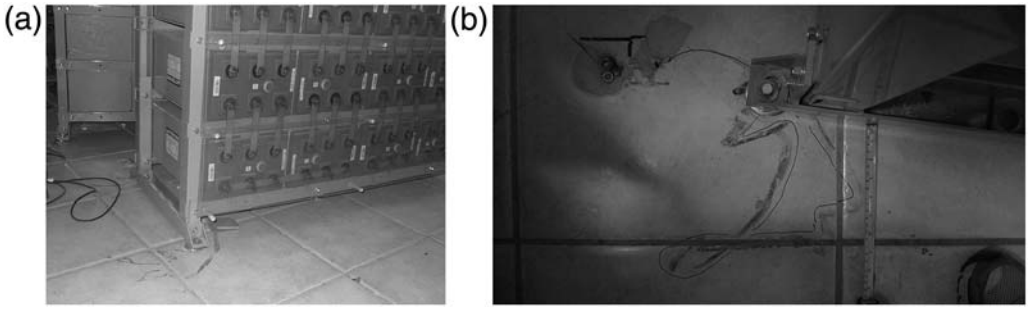

Figure 5. (a) Rack of batteries that was moved across the floor during the mainshock. The near (short) edge of the front rack is aligned roughly north–south, with the closest edge toward the south. (b) Close-up of the scratches left on the tile, including pen marks drawn to indicate the inferred trajectory. (The loop is inferred to have been left by a remnant of the bolt that was dragged as the rack moved.) Two holes can be seen in this photograph: one to the right, where the rack on the right was bolted, and one to the left, where the adjacent rack was bolted. Remnants of a broken bolt can be seen in the hole to the left but are not apparent in the hole to the right.

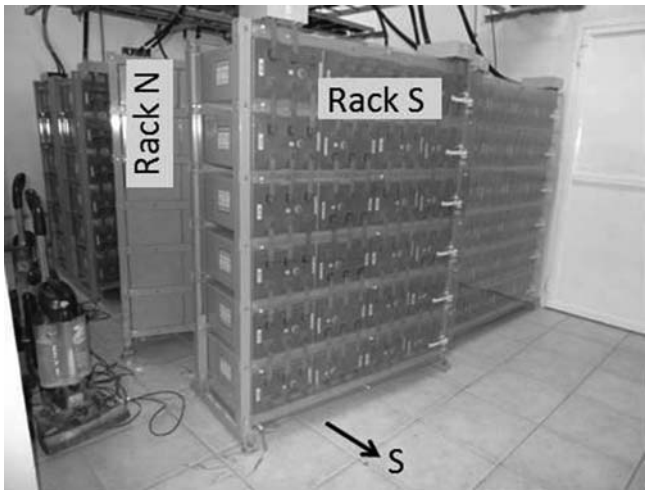

Figure 6. One of the two rooms of battery racks at the HVCV facility. Racks S and N, shown in Figure 5, are in the foreground; apparently identical adjacent racks were not displaced by the earthquake.

The above scenario for the initial response of racks S and N is perhaps open to question, but the details are not critical for an interpretation of the displacement of rack S once it became unbolted. Once the racks were free to move, rack N may have interacted with the neighboring rack on the other side (toward the back of Fig. 5a), but rack S would have moved in response to the initial collision and to the earthquake ground motions. According to this interpretation, the initial southward displacement of rack S, approximately 30 cm, resulted from a combination of collisional forces and the force associated with ground acceleration. During this excursion to the south, rack S also moved approximately 24 cm to the west. This westward component of motion could not have been a consequence of the collision, which would have acted in a perpendicular direction. The two subsequent displacements, approximately 22 and 27 cm are also inferred to be a consequence of ground acceleration.

The scratch marks on the floor reveal no evidence of subsequent rocking after the bolts were broken, which implies a coefficient of friction below 0.33 given the aspect ratio of the rack. The coefficient of friction between the steel legs of the rack and the floor is a key parameter for our analysis; we have not been able to measure it. Established values for the coefficient of friction between steel and other materials are almost universally higher than 0.2, except for extremely slippery materials such as graphite and Teflon. The ceramic tile floor is relatively slippery but presumably less slippery than Teflon. We therefore consider $\mu = 0.15$–0.20 to be a reasonable estimate and use values of 0.15 and 0.20 in our calculations. We can then explore the range of PGA and predominant period of motion that will generate a displacement of 22–27 cm, including an examination of the sensitivity of the results to the assumed coefficient of friction.

We use the results of Taniguchi and Miwa (2007), who consider the slip displacement of a rigid body subjected to sinusoidal horizontal motions as an approximation for motion caused by earthquake shaking. Taniguchi and Miwa (2007) show that, in response to horizontal sinusoidal motion, the maximum relative displacement of a rigid body is given by the following:

$$x_{\sin} = \frac{1}{2}\mu g t_1^2 + \frac{A_{gx} g T^2}{4\pi^2} \sin\frac{2\pi}{T} t_1 + D_1 t_1 + D_2, \quad (1)$$

where

$$D_1 = -\mu g t_0 - \frac{A_{gx} g T}{2\pi} \cos\frac{2\pi}{T} t_0,$$

$$D_2 = \frac{1}{2}\mu g t_0^2 - \frac{A_{gx} g T^2}{4\pi^2} \sin\frac{2\pi}{T} t_0 + \frac{A_{gx} g T t_0}{2\pi} \cos\frac{2\pi}{T} t_0,$$

$$t_0 = \frac{T}{2\pi} \sin^{-1}\frac{\mu}{A_{gx}},$$

$$t_1 = \frac{T}{2\pi A_{gx}} \left\{ -\varphi + \sqrt{\varphi^2 + 2A_{gx}\left[\phi + A_{gx}\left(1 - \frac{\pi^2}{2}\right)\right]} \right\}, \text{ and}$$

$$\varphi = \mu - \pi A_{gx},$$

$$\phi = \mu \sin^{-1}\frac{\mu}{A_{gx}} + A_{gx} \cos\left(\sin^{-1}\frac{\mu}{A_{gx}}\right), \quad (2)$$

where $A_{gx}g$ is the peak acceleration and T is the period. We use equation (1) to calculate x_d for $A_{gx} = 0.1 - 1.5g$ and $T = 0.1 - 1.3$ s, assuming μ values of 0.15 and 0.20.

A further consideration is that, as discussed by Taniguchi and Miwa (2007), predicted slip from input sinusoidal motions, $x_{\sin}$, will differ from predicted slip from earthquake ground motions. On average, the mean ratio between exact displacement and $x_{\sin}$ is approximately 1. That is, 50% of earthquakes with a given A_{gx} are expected to produce a horizontal displacement greater than $x_{\sin}$. Considering 104 earthquake records from sites around Japan, Taniguchi and Miwa (2007) determine the probability density function for a slip ratio, β_{prob}, for including the aspect of earthquake shaking complexity that elongates or shortens the displacement relative to that predicted for input sinusoidal acceleration:

$$x_{\text{eq}} = \beta_{\text{prob}} \cdot x_{\sin}. \quad (3)$$

Using the 104 recordings, Taniguchi and Miwa (2007) derive values of β_{prob} of 1.84 and 2.32 corresponding to probabilities of nonexceedance of 90% and 95%, respectively. That is, if we start with the observed displacement due to an earthquake, x_{eq}, the target displacement we seek to match using equation (1) is $x_{\text{eq}}/\beta_{\text{prob}}$, where we choose β_{prob} for a desired probability of nonexceedance. Thus, to obtain a more statistically rigorous estimate of acceleration due to earthquake shaking, A_{gx}^{eq}, we should consider a target displacement of (22–27 cm)/1.84 to obtain an estimate of A_{gx}^{eq} with a 90% probability of nonexceedance, or (22–27 cm)/2.32 for a 95% probability of nonexceedance. We will use a target displacement of 12–15 cm to estimate A_{gx}^{eq} with a 90% probability of nonexceedance. The choice of a 90% probability of exceedance is arbitrary; we consider it a more reasonable,

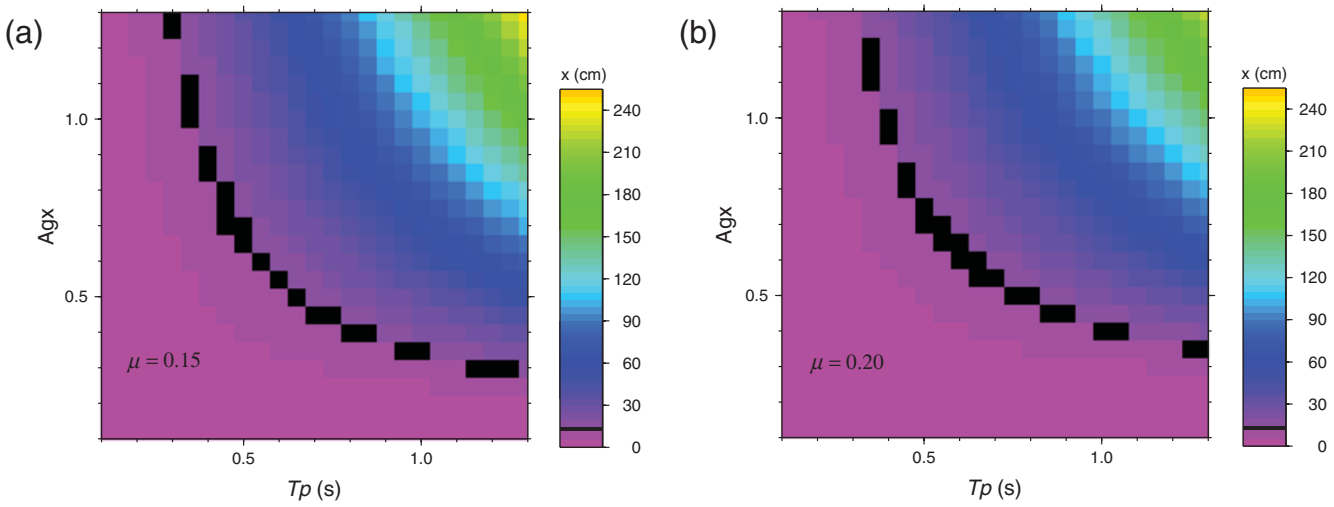

Figure 7. Predicted displacement in cm (color scale indicated) as a function of predominant period of shaking, Tp, and peak acceleration ($A_{gx}g$) for μ values of (a) 0.15 and (b) 0.20. Black swath indicates values that predict maximum displacement values of 12–15 cm, the target displacement to estimate A_{gx}^{eq} with a 90% probability of nonexceedance.

conservative estimate than an estimate corresponding to a 50% probability of exceedance, which has a significant chance of overestimating the true accelerations.

The results shown in Figure 7 reveal that the range of A_{gx}/Tp values that predict a displacement of 12–15 cm do not differ significantly for the assumed values of μ. (Tp is the dominant period of ground acceleration.) In both cases, A_{gx} is upwards of $0.7g$ for $Tp = 0.5$ s, a value that is consistent with the longest-period site response peak inferred from weak-motion recordings. Given the proximity of the mainshock to the site, it is likely that mainshock ground motions were controlled by longer period energy. We consider the range 0.5–1 s to be a reasonable range for Tp. This range corresponds to A_{gx}^{eq} values of roughly 0.3–$0.7g$ for the values of μ considered. We note that the results do not vary significantly for $\mu = 0.15$ versus 0.20.

A final consideration is that the vertical component of slip can effectively reduce or increase the acceleration of gravity. At this site, aftershock recordings reveal that the horizontal components of motion are systematically (and typically) amplified relative to the vertical component by a factor of approximately 2 over a frequency range of 0.4–10 Hz (Fig. 8). As noted by Taniguchi and Miwa (2007), the effects of varying vertical acceleration on the body will have minimal contribution to the displacement given the short time a body is in motion. To provide an adequate safety margin for the predictions of displacement for a given ground motion, Taniguchi and Miwa (2007) assume a monotonous reduction in friction due to vertical acceleration. Considering 144 accelerograms with peak horizontal accelerations scaled to 9 m/s^2, they calculate that introducing a monotonous reduction in friction increases the displacement on average by

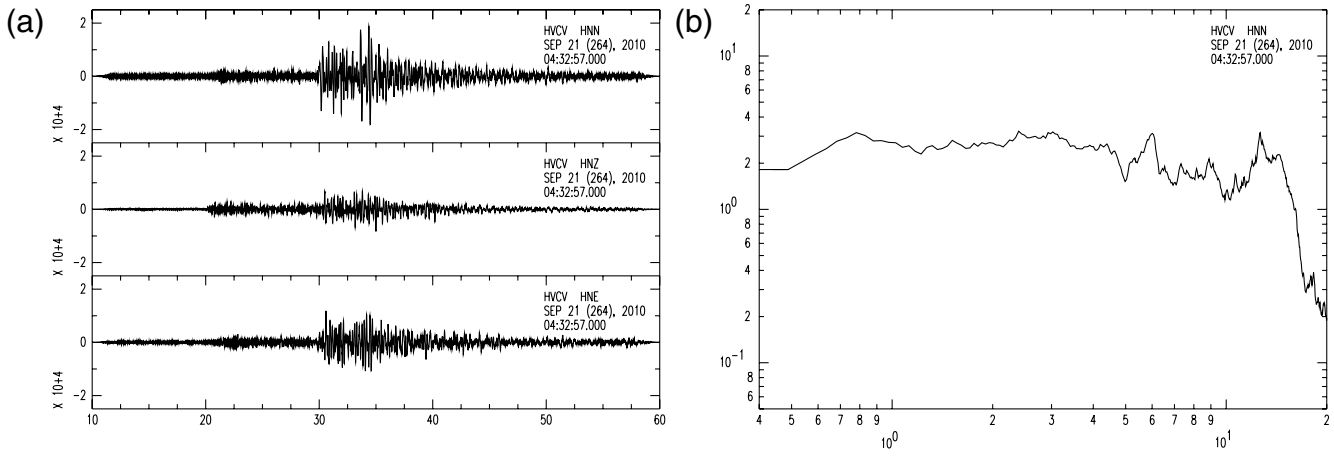

Figure 8. (a) Three components (counts versus time in seconds) of ground motion (north–south, top; vertical, middle; east–west, bottom) for an M 4.4 aftershock recorded at HVCV. (b) North–south/vertical Fourier spectral ratio as a function of frequency.

19%. For a body on a ground floor, the nominal coefficient of friction, μ', is given by

$$\mu' = \mu[1 - \mathrm{PVGA}(\sigma/g)], \quad (4)$$

where PVGA is the peak vertical ground acceleration and σ is the standard deviation of the ratio of the vertical ground acceleration to the peak vertical ground acceleration at the instant of peak horizontal shaking.

In this study, we are not seeking to predict displacement for a given ground motion but rather to infer ground motion for a given displacement. The effects of varying vertical acceleration, which could either increase or decrease effective friction, are unknown but will introduce an additional factor of uncertainty.

To explore the possible effect of vertical accelerations, we assume $\sigma = 0.46$ and the vertical acceleration, PVGA, to be 0.5 horizontal PGA, following Taniguchi and Miwa (2007). Assuming a horizontal PGA of $0.6g$ and vertical acceleration monotonically lowers μ', equation (3) yields $\mu' = 0.86\mu$. If we lower our estimates of μ from 0.15 and 0.20 accordingly (i.e., to 0.13 and 0.17, respectively), the range of inferred A_{gx} values is lowered only slightly (Fig. 9). For example, for $Tp = 0.5$ s, the A_{gx} value that predicts a displacement of 15 cm is $0.65g$ for $\mu' = 0.13$ versus 0.70 for $\mu = 0.15$. As discussed by Taniguchi and Miwa (2007), the target displacement also changes if one considers the effects of vertical base acceleration. For 90% probability of exceedance, the target displacement is 13.0–16.0 cm (i.e., (22–27 cm)/1.69). Given the limitations in the precision of the estimated displacements, this difference is not consequential.

We now return to a consideration of the acceleration that would have been required to break the bolts. Considering the total moment acting about one bolt, one arrives at the following equation for the minimum moment that would be needed to break the bolt:

$$m(A_{gx}g)(H/2) - mg(W/2) = 2\sigma_t(\pi r^2)W, \quad (5)$$

where m is the mass, $A_{gx}g$ is the acceleration, H is the rack height, W is the rack width, and σ_t is the tensile strength of the bolt. The bolts found on the floor were ¼ inch in diameter; we assume similar bolts were used for all of the racks. Assuming a nominal tensile strength (60 kpsi; 4.14×10^8 Pa) for a ¼ inch bolt, one can estimate an upper bound for the PGA of $0.83g$. This bound is consistent with the analysis of rack S displacement; the bound is also consistent with the observation that other racks in the room did not move as a result of the inferred PGA.

Shaking Intensity at the Digicel Building Facility

A second case of rigid body displacement during the Haiti earthquake is documented by Goodno *et al.* (2011): an unanchored cabinet that was shifted across a concrete floor in a commercial building located at 18.53273 N, −72.32324 W (see Fig. 1a). Like the battery racks at HVCV, this cabinet was located at the ground level in a well-built commercial structure that sustained some structural damage but not catastrophic damage or collapse.

Unlike the "battery gram", the documented displacement at the Digicel Building (DB) provides only an indication of the total displacement and not a complete trajectory of the motion. We therefore have to assume that the cabinet was shifted in response to the strongest pulse of acceleration. For this case, we consider a target displacement of ≈7 cm (12.7/1.84) to obtain an estimate of A_{gx}^{eq} with a 90% probability of nonexceedance. In this case, the coefficient of friction is higher because the floor is concrete rather than tile; we assume a μ value of 0.45. Assuming the same range of Tp, we find that A_{gx}^{eq} values of roughly 0.3–0.55g predict a target displacement of

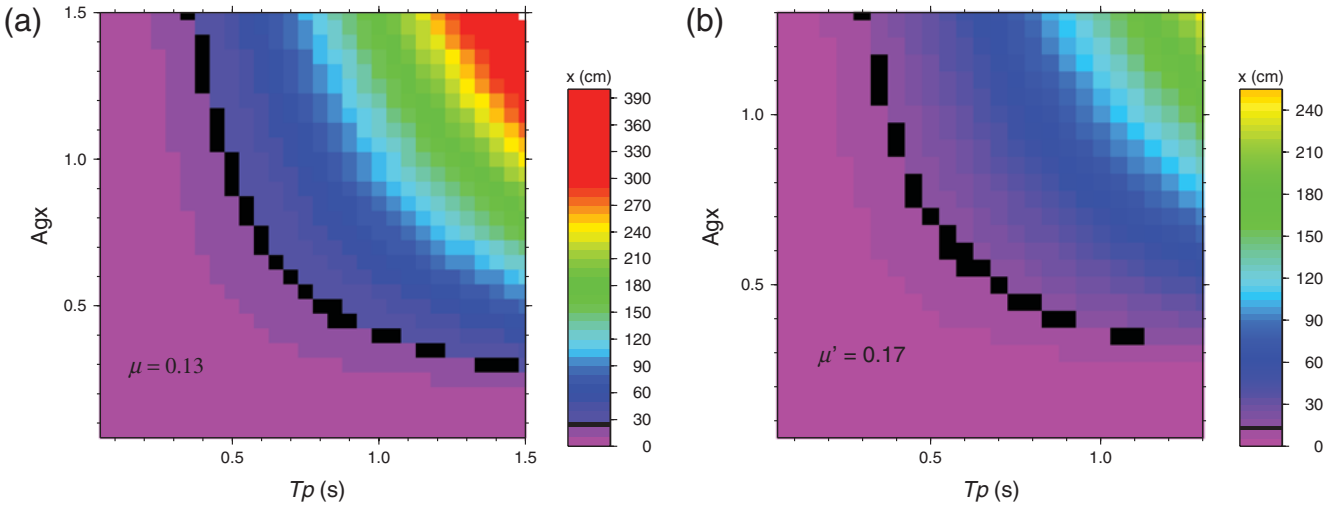

Figure 9. Predicted displacement in cm (color scale indicated) as a function of predominant period of shaking, Tp, and peak acceleration ($A_{gx}g$) for μ' values of (a) 0.13 and (b) 0.17. Black swath indicates values that predict maximum displacement values of 12–15 cm, the target displacement to estimate A_{gx}^{eq} with a 90% probability of nonexceedance.

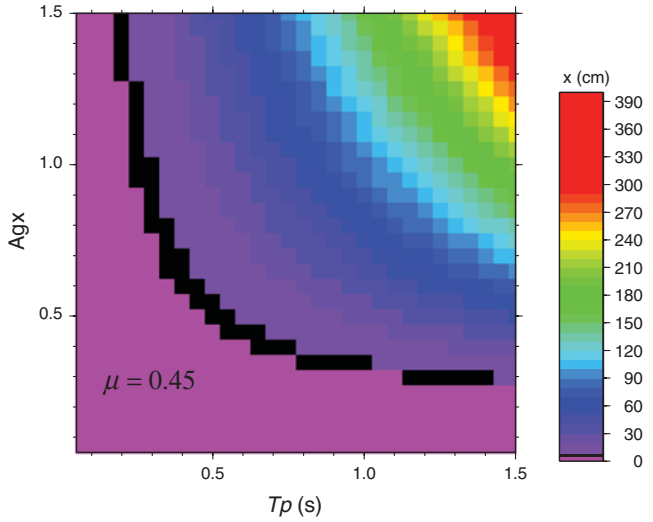

Figure 10. Displacements corresponding to the range of Tp and A_{gx} values are shown for an assumed $\mu = 0.45$. A_{gx} values in the range 0.3–0.55g match the target displacement appropriate for the displaced USB cabinet at the DB site (see fig. 4 of Goodno *et al.*, 2011).

5–8 cm (Fig. 10). Although a more imprecise estimate, our analysis suggests an A_{gx}^{eq} of approximately 0.4g, a severe level of shaking, but slightly lower than the inferred shaking intensity at HVCV. The DB is situated toward the foot of a low ridge, the elevation of which is approximately 15 m higher than the terrain on either side. No aftershock recordings are available from this site.

Comparison with General Assessment of Macroseismic Effects

In the absence of instrumental strong-motion data, we compare our results with the PGA estimated based on generalized assessments of damage and other effects. At the DB site, Goodno *et al.* (2011) estimate a PGA of 0.3–0.47g based on established general correlations between damage and shaking severity. Our quantitative estimate of 0.4g (0.33–0.55g) is consistent with their result (Table 1).

There is no independent assessment of PGA or MMI at HVCV, but we can consider our results in light of observed macroseismic effects at this location and elsewhere. As discussed in the introduction, very poorly built buildings adjacent to the site sustained catastrophic collapse, while the apparently very well-built Voila facility sustained significant nonstructural and light structural damage. These effects are, we conclude, generally consistent with MMI VIII, the indicators for which include extensive damage to unreinforced masonry, toppling of chimneys and monuments, and fall of loose partition walls. According to correlations established from instrumental data in California, MMI VIII corresponds to PGA values of 0.34–0.65g (Wald *et al.*, 1999), which are again highly consistent with our quantitative estimate.

Given the availability of weak-motion amplification factors at HVCV, we can further consider the implications of our results for the severity of shaking in the parts of Port-au-Prince that experienced less severe damage (i.e., tan regions in Fig. 1a). Analysis of aftershocks recorded across the array reveals an average weak-motion PGA amplification of 3.6 at station HVCV relative to hard-rock sites, with suggested resonance peaks at 2–3 Hz and 5–6 Hz (Hough *et al.*, 2010, 2011). PGA amplification at HVCV relative to sites in the valley is a factor of ≈2. Given an estimated mainshock PGA of 0.5 ± 0.2g and assuming linearity of amplification, we can estimate approximate PGA values of 0.15–0.35g in the valley (e.g., HBME and HVGZ) and 0.08–0.19g at hard-rock sites (HCEA) to the south in the mountainous area south of Port-au-Prince.

As noted, based on the consideration of documented effects at the structures shown in Figure 2, we conclude that MMI V–VI is a reasonable assignment for the areas that experienced relatively moderate damage. Wald *et al.* (1999) infer PGA ranges of 3.9%–9.2%g for MMI V and 9.2%–18%g for MMI VI for earthquakes in California. McNamara *et al.* (2012) show that *S*- and *Lg*-wave attenuation in Hispaniola is comparable to attenuation in California. Based on a general assessment of macroseismic effects, we thus conclude that PGA values of approximately 0.1–0.18g are a reasonable estimate for the shaking severity in parts of Port-au-Prince where damage was relatively moderate. The estimate from our quantitative analysis, 0.15–0.35g, is higher but overlaps with this range; we further note that the quantitative estimate is imprecise due to uncertainties in both the mainshock PGA value at HVCV and the estimated amplification factor.

Table 1
Comparison of Results of This Study with Those from Goodno *et al.* (2011) and from General Damage Assessment

Location/Station	Damage	PGA (%g) (This Study)	MMI/PGA	Estimated Amplitude	Consistency
HVCV	Severe*	0.3–0.7	VIII (0.34–0.65)†	3.6	Excellent
HBME	Moderate*	0.15–0.35	V–VI (0.1–0.18)*	2.0	Good
HCEA	Light*	0.08–0.19	NA	1.0	NA
DB	Major†	0.33–0.55	0.3–0.47†	NA	Very good

*This study compared with Goodno *et al.* (2011).
†This study compared with general damage assessment.

One can additionally consider shaking levels predicted from ground-motion prediction equations (GMPEs) established for other tectonically active, and presumably analogous, regions. Recently developed relations predict an average PGA on stiff-soil (NEHRP class C) sites of approximately 0.15*g* for an *M* 7.0 earthquake at 20-km distance (e.g., Campbell and Bozorgnia, 2008). We note that predicted PGA values from GMPEs provide only a rough estimate of shaking. In this case, among other issues, it is not clear what distance is appropriate, because the primary mainshock moment release was primarily to the west of the epicenter and the extent of mainshock rupture toward the east of the epicenter is not well constrained.

The above considerations, as well as the lack of substantial damage to over half of the houses in Port-au-Prince despite pervasively poor construction, suggest that much of Port-au-Prince experienced relatively moderate mainshock ground motions on the order of $\approx 0.2g$, not levels commensurate with MMI values of VIII or above. Locally higher shaking levels were experienced at sites with significant local amplification.

Discussion and Conclusions

We have presented a detailed forensic analysis of two cases of documented rigid body displacement to obtain quantitative estimates of the severity of ground motions in Port-au-Prince during the 12 January 2010 Haiti earthquake. From detailed analysis of the batterygram record observed at station HVCV, we estimate a range of mainshock PGA values of 0.3–0.7*g* at the location where aftershock recordings reveal the highest local amplifications among the recording sites deployed by Hough *et al.* (2010) and where a swath of high damage occurred. Because this level of shaking corresponds to a 90% probability of nonexceedance, this estimate is considered to be conservative. Combining this estimate with the weak-motion amplification factors estimated by Hough *et al.* (2011), we estimate a PGA of approximately 0.2*g* for the parts of the central Port-au-Prince metropolitan region that experienced relatively moderate damage. This estimate is relatively imprecise, but it is consistent with the shaking intensity estimated from a general assessment of macroseismic effects and from GMPEs. We thus conclude that mainshock shaking severity was approximately MMI VI in much of Port-au-Prince (i.e., away from significant sediment-induced or topographic amplification effects) and approximately MMI VIII at sites of strongest local amplification.

The results generally confirm the conclusion based on weak-motion data that local amplifications, in some cases associated with topographic effects, increased the shaking intensity by approximately two units from MMI VI to VIII. A future rupture of the EPGF segment closest to Port-au-Prince is expected to generate higher near-field ground motions within the city, by virtue of proximity and possibly directivity, than those generated by the 2010 earthquake. (The directivity of the 2010 rupture was primarily to the west, away from Port-au-Prince.) Ground motions from such an event are expected to be especially severe at sites with strong local amplification. More generally, our results illustrate how documented horizontal rigid body displacement during earthquakes can be used to obtain quantitative estimates of PGA in the absence of instrumental recordings.

Data and Resources

Aftershock recordings used to estimate weak-motion amplification factors are available through the Incorporated Research Institutions for Seismology Data Management Center (IRIS DMC) (http://www.iris.edu/dms/dmc, last accessed May 2012); a subset of larger aftershock recordings is also available at http://pasadena.wr.usgs.gov/office/hough/DATA/ (last accessed May 2012), although this site is not a permanent repository. High-resolution photographs are available on request from the author. The damage distribution data is described by Voigt *et al.* (2011).

Acknowledgments

The authors express their appreciation to Gerard Laborde and Gregory Domond of the Voila Corporation for their support, without which the deployment, in general, and this investigation, in particular, would not have been possible. We also thank Mehmet Celebi and Robert Dollar for constructive reviews that significantly improved the manuscript; Rasool Anooshehpoor for constructive criticism and suggestions; and Martin Chapman and Diane Doser for editorial stewardship of the journal. The research was supported by the U.S. Agency for International Development (USAID) Office of Foreign Disaster Assistance (OFDA).

References

Atkinson, G., and D. Wald (2007). Modified Mercalli intensity: A surprisingly good measure of ground motion, *Seismol. Res. Lett.* **78,** 362–368.

Bommer, J. J., and J. E. Alarcon (2006). The prediction and use of peak ground velocity, *J. Earthquake Eng.* **10,** 1–31.

Calais, E., A. Freed, G. Mattioli, F. Amelung, S. Jonsson, P. Jansma, S-H. Hong, T. Dixon, C. Prepetit, and R. Momplasir (2010). Transpressional rupture of an unmapped fault during the 2010 Haiti earthquake, *Nat. Geosci.* **3,** 794–799, doi: 10.1038/NGEO992.

Calais, E., Y. Mazabraud, B. M. de Lepinay, P. Mann, G. Mattioli, and P. Jansma (2002). Strain partitioning and fault slip rates in the northern Caribbean from GPS measurements, *Geophys. Res. Lett.* **29,** no. 18, 4 pp., doi: 10.1029/2002GL015397.

Campbell, K. W., and Y. Bozorgnia (2008). NGA ground motion model for the geometric mean horizontal component of PGA, PGV, PGD, and 5% damped linear elastic response spectra for periods ranging from 0.01 to 10 s, *Earthq. Spectra* **24,** 139–171.

Choi, B., and C. C. D. Tung (2001). Newmark's formula for estimating sliding displacement of an unanchored body subjected to earthquake excitation, in *Proc. Structural Mechanics in Reactor Technology (SMiRT) 16 Conference*, Washington, D.C., 12–17 August 2001, Paper No. 1987.

Goodno, B. J., N. C. Gould, P. Caldwell, and P. L. Gould (2011). Effects of the January 2010 Haitian earthquake on selected electrical equipment, *Earthquake Spectra*, **27,** S251–S276.

Hayes, G. P., R.W. Briggs, A. Sladen, E. J. Fielding, C. Prentice, K. Hudnut, P. Mann, F. W. Taylor, A. J. Crone, R. Gold, T. Ito, and M. Simons (2010). Complex rupture during the 12 January 2010 Haiti earthquake, *Nat. Geosci.* **3,** 800–805, doi: 10.1038/NGEO977.

Hinzen, K.-G. (2009). Simulation of toppling columns in archaeoseismology, *Bull. Seismol. Soc. Am.* **99,** no. 5, 2855–2875, doi: 10.1785/0120080241.

Hough, S. E., J. R. Altidor, D. Anglade, H. Benz, W. Ellsworth, D. Given, J. Hardebeck, M. G. Janvier, J. Z. Maharrey, Y. Mazabraud, D. McNamara, B. M. de Lepinay, M. Meremonte, B. S.-L. Mildor, C. Prepetit, and A. Yong (2010). Localized damage associated with topographic amplification during the 12 January 2010 *M* 7.0 Haiti earthquake, *Nat. Geosci.* **3,** 778–782.

Hough, S.E., J. R. Altidor, D. Anglade, D. Given, M. G. Janvier, J. Z. Maharrey, M. Meremonte, S.-L. Mildor, C. Prepetit, and A. Yong (2011). Site response and site characterization in Port-au-Prince, Haiti, *Earthquake Spectra* **27,** S137–S155.

Mann, P., G. Draper, and J. F. Lewis (1991). An overview of the geologic and tectonic development of Hispaniola, *Spec. Pap. Geol. Soc. Am.* **262,** 1–28.

McNamara, D., M. Meremonte, J. Z. Maharrey, S-L. Mildor, J. R. Altidor, D. Anglade, S. E. Hough, D. Given, H. Benz, L. Gee, and A. Frankel (2012). Frequency Dependent Seismic Attenuation within the Hispaniola Island Region of the Caribbean Sea, *Bull. Seism. Soc. Am.* **102,** 773–782, doi: 10.1785/0120110137.

Ministere de l'Ecologie, du Developpement et de l'Amenagement Durable (MEDAD) (2007). *Le Seisme de Chuetsu-Oki (Japon) du 16 Juillet 2007*, Association Francaise du Genie Parasismique, Paris.

Miyamoto, H. K., A. S. J. Gilani, and K. Wong (2011). Massive damage assessment program and repair and reconstruction strategy in the aftermath of the 2010 Haiti earthquake, *Earthquake Spectra* **27,** S219–S237, doi: 10.1193/1.3631293.

Newmark, N. M. (1965). Effets of earthquakes on dams and embankments: Fifth Rankine Lecture, *Geotechnique* **15,** 139–160.

Sanchez-Sesma, F. J. (1985). Diffraction of elastic *SH* waves by wedges, *Bull. Seismol. Soc. Am.* **75,** 1435–1446.

Taniguchi, T., and T. Miwa (2004). Slip displacement analysis of freestanding rigid bodies subjected to earthquake motions, in *Proc. 13th World Conference of Earthquake Engineering*, Vancouver, Canada, August 1–6, Paper No. 437.

Taniguchi, T., and T. Miwa (2007). A simple procedure to approximate slip displacement of freestanding rigid body subjected to earthquake motions, *Earthquake Eng. Struct. Dynam.* **36,** no. 4, 481–501, doi: 10.1002/eqe.639.

Voigt, S., T. Schneiderhan, A. Twele, M. Gahler, E. Stein, and H. Mehl (2011). Rapid damage assessment and situation mapping: Learning from the 2010 Haiti earthquake, *Programmetric Eng. Remote Sens.* **77,** 923–931.

Wald, D. J., V. Quitoriano, T. H. Heaton, and H. Kanamori (1999). Relationships between peak ground acceleration, peak ground velocity, and modified Mercalli intensity in California, *Earthquake Spectra* **15,** 557–564.

U.S. Geological Survey
525 S. Wilson Avenue
Pasadena, California 91106
(S.E.H.)

Department of Civil Engineering,
Tottori University
4-101 Koyama-Minami
Tottori 680-8552, Japan
(T.T.)

Bureau des Mines et de l'Energie
Rue de Jacques, Delmas 31
Port-au-Prince, Haiti
(J.-R.A.)

Manuscript received 8 February 2012